

# Analysing spatially extended high-dimensional chaos by recurrence plots

Norbert Marwan<sup>a</sup>, Jürgen Kurths<sup>a,b,c</sup>, Saskia Foerster<sup>d</sup>

<sup>a</sup>*Potsdam Institute for Climate Impact Research, 14412 Potsdam, Germany*

<sup>b</sup>*Humboldt Universität zu Berlin, Institut für Physik, Germany*

<sup>c</sup>*Nizhny Novgorod State University, Department of Control Theory, Nizhny Novgorod, Russia*

<sup>d</sup>*GFZ German Research Centre for Geosciences, Section 1.4 Remote Sensing, Telegrafenberg, 14473 Potsdam, Germany*

---

## Abstract

Recurrence plot based measures of complexity are capable tools for characterizing complex dynamics. In this letter we show the potential of selected recurrence plot measures for the investigation of even high-dimensional chaos. We apply this method on spatially extended chaos, such as derived from the Lorenz96 model and show that the recurrence plot based measures can qualitatively characterize typical dynamical properties such as chaotic or periodic dynamics. Moreover, we demonstrate its power by analyzing satellite image time series of vegetation cover with contrasting dynamics as a high-dimensional example from the real world.

*Keywords:* spatially extended chaos, recurrence plot, Lorenz96, remote sensing

*PACS:* 05.45.Jn, 05.45.Tp, 89.60.-k

---

## 1. Introduction

Recurrence plots (RPs) are powerful tools for the study of the complex behavior of dynamical systems [1]. They represent time points of recurring states even of high-dimensional phase space trajectories. Quantitative extensions, such as recurrence quantification analysis and recurrence networks, enable the investigation of dynamical transitions and regime changes, the quantitative characterization of the dynamics, or the detection of phase synchronization [2–4]. The practical and powerful use of RP based methods has been demonstrated by their growing and interdisciplinary application, such as for cardiovascular health diagnosis, behavioral, cognitive and neurological studies, studying fluid dynamics and plasma, analyzing optical effects, material health monitoring, palaeoclimate regime change detection, etc. [5–12]. In general, such studies have so far been restricted to rather low-dimensional systems. However, when studying the complex behavior of real world systems, we often end up on extended complex systems, and the question arises whether the RP based tools

---

*Email address:* marwan@pik-potsdam.de (Norbert Marwan)

can be applied on high-dimensional systems, such as exhibiting high-dimensional chaos. So far, the ability of RP based methods for studying high-dimensional chaos has not yet been demonstrated, although it was already used to investigate spatial recurrences [13–15] and spatio-temporal chaos in turbulence and a reaction-diffusion system [16, 17]. Moreover, the classic characterization of complex dynamics by using correlation dimension and Lyapunov exponents requires very long time-series [18] or the knowledge of the differential equations of the system which are in practical examples not known. The study of extended spatio-temporal dynamics is even more complicated and challenging.

In this letter we demonstrate the potential of RP based measures of complexity for identifying hardly accessible extended spatio-temporal dynamics and for characterizing high-dimensional chaos. We will use the Lorenz96 model [19–21] which is a paradigmatic system for extended complex spatio-temporal chaotic dynamics and was systematically studied by Karimi et al. [22] and apply the method on an example of a satellite time series imagery.

## 2. The Lorenz96 model

The Lorenz96 model is a conceptual time-continuous linear lattice model that was developed to demonstrate fundamental aspects of weather predictability [19]:

$$\frac{dx_k}{dt} = (x_{k+1} - x_{k-2})x_{k-1} - x_{k-1} + f \quad (1)$$

for  $k = 1, \dots, N$ , with a constant external forcing  $f$ , and with periodic boundary conditions  $x_{N+1} = x_1$ . Depending on the system size  $N$  and the forcing  $f$ , the dynamics on the lattice can be periodic or chaotic and can exhibit a high dimensionality [22]. Therefore, this model is very appropriate for our study.

For integrating Eq. (1) we use a Runge-Kutta integration of 4th order with time step  $\delta t = 1/64$ . In order to remove transients, we neglect the first 10,000 values from each  $x_k(t)$ . In the numerical experiments discussed below, we will use 20 slightly varying initial conditions for each selected setting of  $N$  and  $f$ .

In our study we consider  $f = 5$ . Then, for example, for  $N = 38$ , we find periodic dynamics, but for  $N = 47$ , the dynamics is chaotic (Fig. 1).

The change of the dynamical regimes with systems size  $N$  can be measured by the maximal Lyapunov exponent  $\lambda_{\max}$  and the Kaplan-Yorke dimension  $D_{KY}$ , which can be calculated using the Wolf algorithm for  $\lambda$  [23] and the Kaplan-York algorithm for  $D_\lambda$  [24] (here we used 200,000 iterations for this calculation). Increasing the system size from  $N = 10$  to  $N = 50$  reveals a periodic alternation between periodic and chaotic dynamics by periodic variations of  $\lambda_{\max}$  (Fig. 2a). The dimension of the system as measured by  $D_{KY}$  is increasing by trend (Fig. 3a). The calculation of  $\lambda$  and  $D_{KY}$  is expensive for such high-dimensional systems. Moreover, for accurate values we need very long time series (here, even for  $N = 200,000$  we find some spread in the results of  $\lambda_{\max}$  and  $D_{KY}$ ).

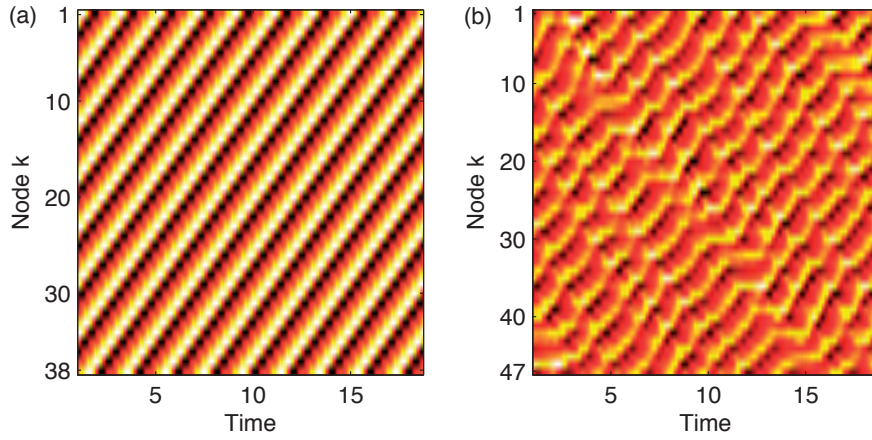


Figure 1: Space-time representation of  $x_k(t)$  for  $f = 5$  and system size of (a)  $N = 38$  and (b)  $N = 47$ , showing periodic and chaotic dynamics.

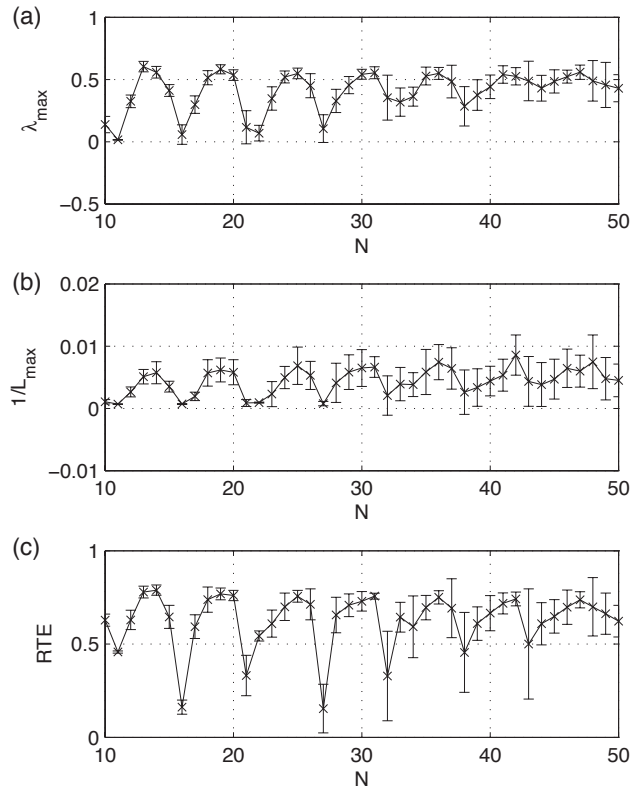


Figure 2: (a) Maximal Lyapunov exponent  $\lambda_{\max}$  for the Lorenz96 model with different system size  $N$ . The RP based measures (b)  $1/L_{\max}$  and (c) RTE reveal a similar variation with the  $N$  as  $\lambda_{\max}$ . Averaged values for 20 different initial states are presented. The standard deviation of the measures for the different initial conditions are presented by the error bars.

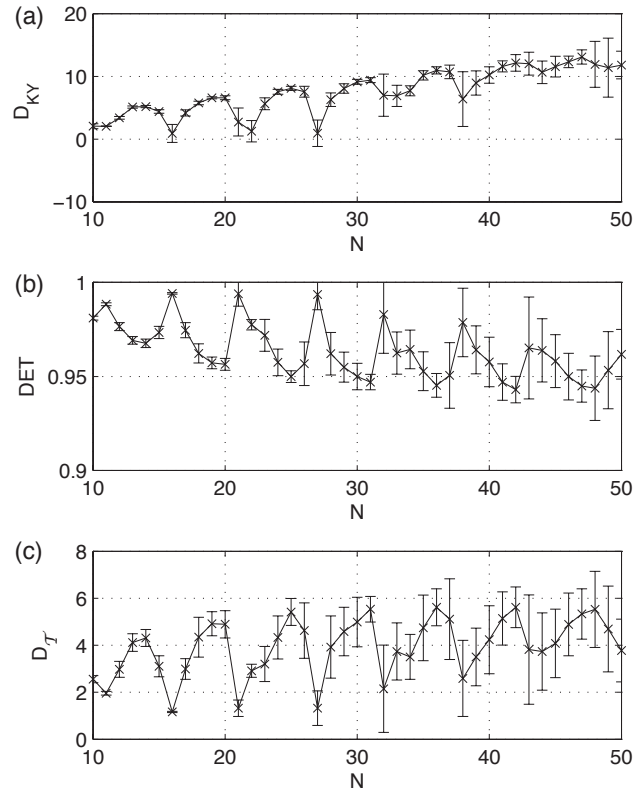


Figure 3: (a) Kaplan-Yorke dimension  $D_{KY}$  for the Lorenz96 model with different system size  $N$ . The RP based measures (b) DET and (c)  $D_T$  reveal a similar variation with the  $N$  as  $D_{KY}$ . Averaged values for 20 different initial states are presented. The standard deviation of the measures for the different initial conditions are presented by the error bars.

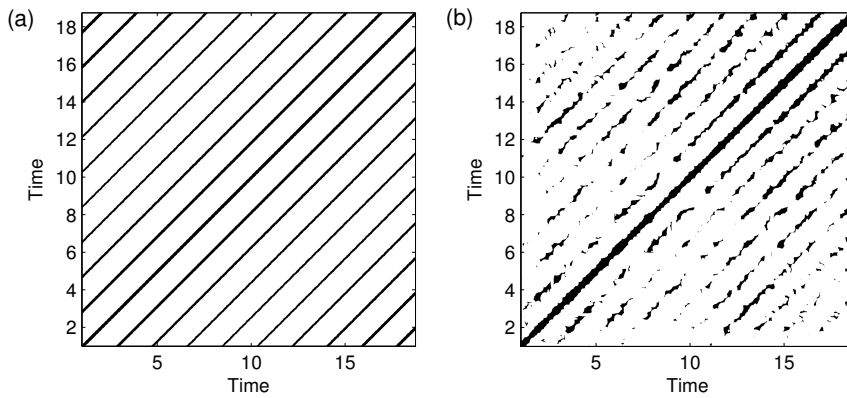


Figure 4: Recurrence plots of the Lorenz96 system  $x_k(t)$  for  $f = 5$  and system size of (a)  $N = 38$  and (b)  $N = 47$ , showing periodic and chaotic dynamics.

### 3. Recurrence plot analysis

RP quantification may be suitable for a simpler estimation of the dynamical properties. A RP  $R_{i,j} = \Theta(\varepsilon - \|\vec{x}_i - \vec{x}_j\|)$  is a binary matrix  $\mathbf{R}$  representing the time points  $j$  when a state  $\vec{x}_i$  at time  $i$  recurs [2] (Fig. 4). The recurrence criterion is usually defined as a spatial distance between two states  $\vec{x}_i$  and  $\vec{x}_j$  is falling below a threshold  $\varepsilon$ . Besides the ability to discuss the visual aspect of a RP, several quantification approaches are based on this matrix. The diagonal line structures in a RP correspond to periods of parallel evolution of two segments of the phase space trajectory. The scaling of the length distribution of such lines is related to the  $K_2$  entropy. A good proxy for this is measuring the inverse of the length of the longest diagonal line  $1/L_{\max}$ , with

$$L_{\max} = \arg \max_l H_D(l), \quad (2)$$

and  $l$  the length of the diagonal lines, and  $H_D(l)$  the length distribution of diagonal lines in  $\mathbf{R}$  [2].

Based on a heuristic approach, the fraction of recurrence points that form such diagonal lines is a qualitative measure of determinism (DET) [2],

$$DET = \frac{\sum_{l=2}^N l H_D(l)}{\sum_{i,j=1}^N R_{i,j}}. \quad (3)$$

Systems possessing deterministic dynamics are characterized by diagonal lines indicating repeating recurrences within a state (and, hence, higher  $DET$  values).

The vertical empty space between two recurrence points in the RP correspond to Poincaré recurrence times, i.e., the distance  $v$  between recurrence points in a column of  $\mathbf{R}$  [25]. From the distribution  $H_V(v)$  we can derive the *recurrence time entropy* ( $RTE$ ), also called *recurrence period density entropy* [26]

$$RTE = -\frac{1}{\ln V_{\max}} \sum_{v=1}^{V_{\max}} H_V(v) \ln H_V(v). \quad (4)$$

This measure quantifies the extent of recurrences and is related to the Pesin dimension [27].

In the last years, the similarity of the binary, squared matrix  $\mathbf{R}$  with the adjacency matrix of an unweighted, undirected complex network was used to apply complex network measures on recurrence plots in order to quantify the geometrical properties of the system's attractor encoded in the RP [28]. For example, the *transitivity coefficient* ( $\mathcal{T}$ )

$$\mathcal{T} = \frac{\sum_{i,j,k=1}^N R_{j,k} R_{i,j} R_{i,k}}{\sum_{i,j,k=1}^N R_{i,j} R_{i,k} (1 - \delta_{j,k})}. \quad (5)$$

allows the differentiation of regular and irregular dynamics [29]. Moreover,  $\mathcal{T}$  can be used to define a novel dimensionality measure, the *transitivity dimension* ( $D_{\mathcal{T}}$ )

$$D_{\mathcal{T}} = \frac{\log(\mathcal{T})}{\log(3/4)}, \quad (6)$$

allowing the calculation of the dimension without explicit consideration of scaling behaviors. Using the RP, the correlation dimension  $D_2$  can also be derived [30]. However, the advantage of  $D_{\mathcal{T}}$  is that it results directly from the RP without analyzing any scaling behavior depending on the recurrence threshold  $\varepsilon$ .

Although still rather novel, such recurrence quantification is meanwhile widely accepted and applied in different disciplines to study diverse problems. For more details on this methodology we refer to [2, 4, 31, 32].

#### 4. Recurrence analysis of spatially extended chaos

For the application of the RP approach to spatially extended high-dimensional data such as from the Lorenz96 model, we consider each variable as one component of the phase space representation:  $\vec{x}(t) = (x_1(t), x_2(t), \dots, x_N(t))$ . We remove transients by deleting the first 10,000 data points and then downsample the time series by considering only every 2nd value. Then, for only 1,500 time points of the vector  $\vec{x}(t)$  we calculate the RP and the above mentioned measures DET,  $1/L_{\max}$ , RTE, and  $D_{\mathcal{T}}$ . We calculate this set of measures for different system size  $N = [10, 50]$  and repeat the calculation for 20 different initial conditions. For the line based RP measures DET and  $1/L_{\max}$  we choose a minimal line length of two. We apply a Theiler window of length 10 (in units of iteration steps) and a recurrence threshold such that the fraction of recurrences in the RP is 10% (and using the Euclidean norm).

The inverse of the longest diagonal line  $1/L_{\max}$  as well as the RTE reveal a similar alternating variation with  $N$  as  $\lambda_{\max}$  (Fig. 2b,c). The Pearson correlation between these two RP based measures and  $\lambda_{\max}$  is 0.90 (for  $1/L_{\max}$ ) and 0.77 (for RTE). The strong correlation even for the used rather short data segment suggests that these RP based measures are good estimators for studying the divergence behavior of high-dimensional systems.

The DET measure varies between values of 0.94 and 1, indicating the high deterministic nature of the model (Fig. 3b). During the periodic regimes, the DET shows maxima, whereas during the chaotic regime, DET falls to lower values. The transitivity dimension  $D_{\mathcal{T}}$  varies rather similar compared to the Kaplan-Yorke dimension  $D_{KY}$ . It also shows the upward trend with increasing  $N$  (Fig. 3c), but  $D_{KY}$  is in average 2.5 times higher than  $D_{\mathcal{T}}$ . The correlation of  $D_{KY}$  with DET and  $D_{\mathcal{T}}$  is  $-0.78$  and  $0.70$ , respectively.

The recurrence based measures are able to reveal the dynamics using very short time series of length 1,500, in comparison to the classic measures where 200,000 iterations and the differential equations had been necessary.

#### 5. Application on satellite time series imagery

For testing the proposed RP quantitative measures on high-dimensional real world data, we used MODIS satellite time series imagery of the extended vegetation index (EVI) of two test sites in NE Spain (centre coordinate  $42.37^\circ\text{N}$ ,  $0.51^\circ\text{E}$ ) and NE Brazil ( $5.00^\circ\text{S}$ ,  $39.50^\circ\text{W}$ ). The test sites are characterized by differently complex vegetation dynamics both in the temporal (inter-annual and intra-annual) and spatial domain as a result of diverse natural

processes and human interactions. Thus, these sites are seen as ideal to study the usefulness of the proposed RP measures in order to objectively quantify and evaluate this complex behavior and decipher changes in vegetation cover dynamics related to land extensification/intensification or climate change and drought. The subhumid Spanish test site shows a pronounced seasonal variation in precipitation and temperature with cold and dry winters and hot and stormy summers, whereas the Brazilian test site located in the so-called drought polygon is characterized by a semiarid climate with distinct dry and wet seasons and rainfall of high temporal and spatial irregularity. The Spanish test site has undergone severe land use changes during the last 50 years with the abandoning of former agricultural areas and subsequent reforestation as well as setting aside of lands from agriculture promoted by the European Agricultural Policy [33]. The Brazilian test site has been more intensively occupied since 1985, when the Federal Government accomplished a land reform leading to the intensification of agricultural and livestock practices. A dense water surface reservoir network has been built in the last decades to mitigate water scarcity problems [34].

The MODIS-Terra MOD13Q1 product used for this real world application is a 16-day composite image of the enhanced vegetation index (EVI) in a sinusoidal projection with a spatial resolution of 250 m. Global MODIS vegetation indices are designed to provide consistent spatial and temporal datasets used for global monitoring of vegetation conditions. The EVI was chosen since it minimizes canopy background variations and maintains sensitivity over dense vegetation. We obtained 316 MOD13Q1 images for the period February 2000 to November 2013 for both the MODIS tiles h18v04 (Spain) and h14v09 (Brazil) from the Land Processes Distributed Active Archive Center (LP DAAC), located at the US Geological Survey (USGS) Earth Resources Observation and Science (EROS) Center ([lpdaac.usgs.gov](http://lpdaac.usgs.gov)).

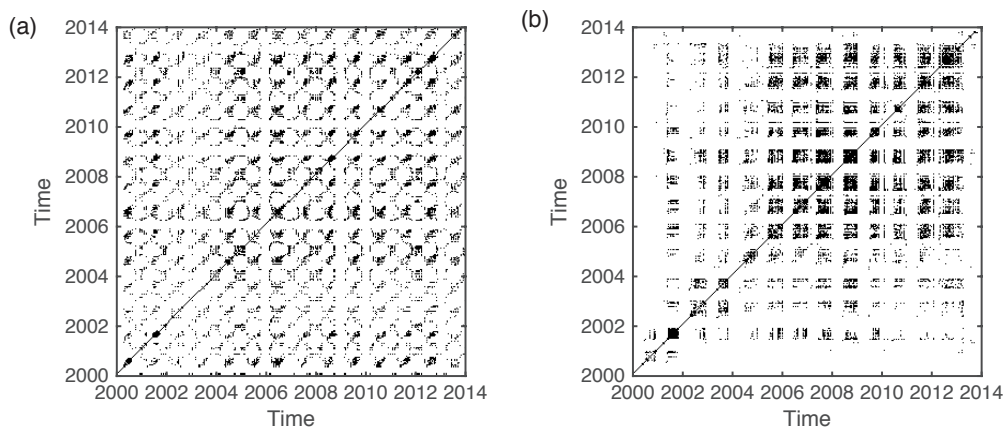


Figure 5: Recurrence plot of a  $5 \times 5 \text{ km}^2$  subarea of the MODIS extended vegetation index (EVI) of test sites in (a) NE Spain and (b) NE Brazil. The selected subarea is situated at the centre point of the study region (see text).

In both regions we consider subareas of  $5 \times 5 \text{ km}^2$  ( $N = 441$  grid points) varying around the centre point by  $0.25^\circ$  and within a range of  $[-0.5^\circ, 0.5^\circ]$  (resulting in 25 subareas for both regions). That way, the subareas contain a mixture of land covers representative for the test

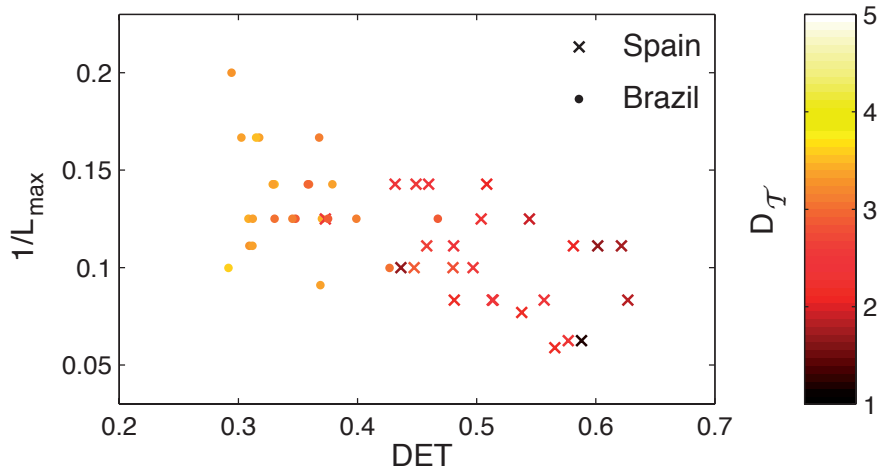


Figure 6: Recurrence quantification measures for the MODIS EVI data for different subareas around the study regions' centre point.

sites. For both regions we visually find periodic patterns in the corresponding RPs, revealing mainly the seasonal variability (Fig. 5). The appearance of the periodic patterns differ for Spain (more line-like patterns) and Brazil (more block-like patterns), indicating substantial differences in the spatial dynamics. The RP quantification by the measures DET,  $1/L_{\max}$ , and  $D_{\mathcal{T}}$  clearly reveals quantitative differences: in Brazil we find a more erratic or chaotic spatio-temporal pattern than in Spain, indicated by lower DET and higher  $1/L_{\max}$  as well as  $D_{\mathcal{T}}$  for Brazil (Fig. 6, Tab. 1). Although the considered subareas consist of information that is a mixed signal of several land cover classes, the difference between Spain and Brazil is consistent for subareas of varying location. These results can be interpreted in such sense that the vegetation (or land use) dynamics in Brazil is probably less regulated and less predictable than in Spain.

Table 1: Median of recurrence quantification measures for the MODIS EVI data (standard deviation in brackets).

	Spain	Brazil
DET	0.51 (0.07)	0.33 (0.04)
$1/L_{\max}$	0.10 (0.03)	0.13 (0.03)
$D_{\mathcal{T}}$	2.35 (0.45)	3.85 (0.41)

## 6. Conclusion

By using the Lorenz96 model as a prototypical example of high-dimensional chaos we have shown that recurrence plot based analysis can be used to investigate high-dimensional chaos from rather short time series and provides insights in the fundamental features of the dynamics, comparable with the Kaplan-York dimension or the Lyapunov exponent.

This study, thus, answers the up to now open question, whether recurrence plots and their quantification is suitable to study high-dimensional chaos. The more systematic study on the limits of the used methods and the necessary length of time series in dependence on the dimension of the system is subject of future work.

Moreover, by applying the method to MODIS satellite time series data we have demonstrated its suitability for the investigation of high-dimensional spatio-temporal dynamics of real world processes. The recurrence analysis has indicated a clear difference in the spatio-temporal vegetation dynamics in a subhumid (Spain) and in a semiarid (Brazil) climate, where the first shows a more regular pattern, whereas the latter is characterized by a more irregular and less predictable behavior.

## **7. Acknowledgement**

We acknowledge support from the DFG and FAPESP (project MA 4759/4-1 and IRTG 1740/TRP 2011/50151-0) and from the Government of the Russian Federation (Agreement No. 14.Z50.31.0033).

## References

- [1] J.-P. Eckmann, S. Oliffson Kamphorst, D. Ruelle, Recurrence Plots of Dynamical Systems, *Europhysics Letters* 4 (9) (1987) 973–977. doi:10.1209/0295-5075/4/9/004.
- [2] N. Marwan, M. C. Romano, M. Thiel, J. Kurths, Recurrence Plots for the Analysis of Complex Systems, *Physics Reports* 438 (5–6) (2007) 237–329. doi:10.1016/j.physrep.2006.11.001.
- [3] R. V. Donner, J. Heitzig, J. F. Donges, Y. Zou, N. Marwan, J. Kurths, The Geometry of Chaotic Dynamics – A Complex Network Perspective, *European Physical Journal B* 84 (2011) 653–672. doi:10.1140/epjb/e2011-10899-1.
- [4] C. L. Webber, Jr., N. Marwan, Recurrence Quantification Analysis – Theory and Best Practices, Springer, Cham, 2015. doi:10.1007/978-3-319-07155-8.
- [5] G. M. Ramírez Ávila, A. Gapelyuk, N. Marwan, T. Walther, H. Stepan, J. Kurths, N. Wessel, Classification of cardiovascular time series based on different coupling structures using recurrence networks analysis, *Philosophical Transactions of the Royal Society A* 371 (1997) (2013) 20110623. doi:10.1098/rsta.2011.0623.
- [6] D. C. Richardson, R. Dale, Looking To Understand: The Coupling Between Speakers’ and Listeners’ Eye Movements and Its Relationship to Discourse Comprehension, *Cognitive Science* 29 (6) (2005) 1045–1060.
- [7] E. D. Eneyew, M. Ramulu, Tool wear monitoring using microphone signals and recurrence quantification analysis when drilling composites, *Advanced Materials Research* 711 (2013) 239–244. doi:10.4028/www.scientific.net/AMR.711.239.
- [8] Z. O. Guimarães-Filho, I. L. Caldas, R. L. Viana, I. C. Nascimento, Y. K. Kuznetsov, J. Kurths, Recurrence quantification analysis of turbulent fluctuations in the plasma edge of Tokamak Chauffage Alfvén Brésilien tokamak, *Physics of Plasmas* 17 (2010) 012303. doi:10.1063/1.3280010.
- [9] M. Tahmasebpour, R. Zarghami, R. Sotudeh-Gharebagh, N. Mostoufi, Characterization of various structures in gas-solid fluidized beds by recurrence quantification analysis, *Particuology* 11 (6) (2013) 647–656. doi:10.1016/j.partic.2012.08.005.
- [10] B. Krese, M. Perc, E. Govekar, Experimental observation of a chaos-to-chaos transition in laser droplet generation, *International Journal of Bifurcation and Chaos* 21 (6) (2011) 1689–1699. doi:10.1142/S0218127411029367.
- [11] I. Konvalinka, D. Xygalatas, J. Bulbulia, U. Schjodt, E. M. Jegindo, S. Wallot, G. Van Orden, A. Roepstorff, Synchronized arousal between performers and related spectators in a fire-walking ritual, *Proceedings of the National Academy of Sciences* 108 (20) (2011) 8514–8519. doi:10.1073/pnas.1016955108.
- [12] J. F. Donges, R. V. Donner, M. H. Trauth, N. Marwan, H. J. Schellnhuber, J. Kurths, Nonlinear detection of paleoclimate-variability transitions possibly related to human evolution, *Proceedings of the National Academy of Sciences* 108 (51) (2011) 20422–20427. doi:10.1073/pnas.1117052108.
- [13] D. B. Vasconcelos, S. R. Lopes, R. L. Viana, J. Kurths, Spatial recurrence plots, *Physical Review E* 73 (2006) 056207. doi:10.1103/PhysRevE.73.056207.
- [14] N. Marwan, J. Kurths, P. Saparin, Generalised Recurrence Plot Analysis for Spatial Data, *Physics Letters A* 360 (4–5) (2007) 545–551. doi:10.1016/j.physleta.2006.08.058.
- [15] T. L. Prado, P. P. Galuzio, S. R. Lopes, R. L. Viana, Spatial recurrence analysis: A sensitive and fast detection tool in digital mammography, *Chaos* 24 (2014) 013106. doi:10.1063/1.4861895.
- [16] Z. O. Guimarães-Filho, I. L. Caldas, R. L. Viana, J. Kurths, I. C. Nascimento, Y. K. Kuznetsov, Recurrence quantification analysis of electrostatic fluctuations in fusion plasmas, *Physics Letters A* 372 (7) (2008) 1088–1095. doi:10.1016/j.physleta.2007.07.088.
- [17] C. Mocenni, A. Facchini, A. Vicino, Identifying the dynamics of complex spatio-temporal systems by spatial recurrence properties, *Proceedings of the National Academy of Sciences* 107 (18) (2010) 8097–8102. doi:10.1073/pnas.0910414107.
- [18] J.-P. Eckmann, D. Ruelle, Fundamental limitations for estimating dimensions and Lyapunov exponents in dynamical systems, *Physica D* 56 (2–3) (1992) 185–187. doi:10.1016/0167-2789(92)90023-G.
- [19] E. N. Lorenz, *Predictability: A problem partly solved*, Vol. 1, ECMWF, Reading, UK, 1996, pp. 1–18.
- [20] E. N. Lorenz, K. A. Emanuel, Optimal Sites for Supplementary Weather Observations: Simulation

- with a Small Model, *Journal of the Atmospheric Sciences* 55 (3) (1998) 399–414. doi:10.1175/1520-0469(1998)055<0399:OSFSW0\$>\$2.0.CO;2.
- [21] D. Pazó, I. G. Szendro, J. M. López, M. A. Rodríguez, Structure of characteristic Lyapunov vectors in spatiotemporal chaos, *Physical Review E* 78 (1) (2008) 016209. doi:10.1103/PhysRevE.78.016209.
- [22] A. Karimi, M. R. Paul, Extensive chaos in the Lorenz-96 model., *Chaos* 20 (4) (2010) 043105. doi:10.1063/1.3496397.
- [23] A. Wolf, J. B. Swift, H. L. Swinney, J. A. Vastano, Determining Lyapunov Exponents from a Time Series, *Physica D* 16 (3) (1985) 285–317. doi:10.1016/0167-2789(85)90011-9.
- [24] J.-P. Eckmann, D. Ruelle, Ergodic theory of chaos and strange attractors, *Review of Modern Physics* 57 (3) (1985) 617–656. doi:10.1103/RevModPhys.57.617.
- [25] E. J. Ngamga, D. V. Senthilkumar, A. Prasad, P. Parmananda, N. Marwan, J. Kurths, Distinguishing dynamics using recurrence-time statistics, *Physical Review E* 85 (2) (2012) 026217. doi:10.1103/PhysRevE.85.026217.
- [26] L. M. Little, P. McSharry, S. J. Roberts, D. A. E. Costello, I. M. Moroz, Exploiting Nonlinear Recurrence and Fractal Scaling Properties for Voice Disorder Detection, *BioMedical Engineering OnLine* 6 (23) (2007) 1–19. doi:10.1186/1475-925X-6-23.
- [27] V. S. Anishchenko, S. V. Astakhov, Poincaré recurrence theory and its applications to nonlinear physics, *Physics-Uspekhi* 56 (10) (2013) 955–972. doi:10.3367/UFNe.0183.201310a.1009.
- [28] N. Marwan, J. F. Donges, Y. Zou, R. V. Donner, J. Kurths, Complex network approach for recurrence analysis of time series, *Physics Letters A* 373 (46) (2009) 4246–4254. doi:10.1016/j.physleta.2009.09.042.
- [29] Y. Zou, R. V. Donner, J. F. Donges, N. Marwan, J. Kurths, Identifying complex periodic windows in continuous-time dynamical systems using recurrence-based methods, *Chaos* 20 (4) (2010) 043130. doi:10.1063/1.3523304.
- [30] P. Grassberger, I. Procaccia, Characterization of strange attractors, *Physical Review Letters* 50 (5) (1983) 346–349. doi:10.1103/PhysRevLett.50.346.
- [31] N. Marwan, How to avoid potential pitfalls in recurrence plot based data analysis, *International Journal of Bifurcation and Chaos* 21 (4) (2011) 1003–1017. doi:10.1142/S0218127411029008.
- [32] N. Marwan, M. Riley, A. Giuliani, C. L. Webber, Jr., *Translational Recurrences – From Mathematical Theory to Real-World Applications*, Vol. 103, Springer, Cham, 2014. doi:10.1007/978-3-319-09531-8.
- [33] T. Lasanta, S. M. Vicente-Serrano, Complex land cover change processes in semiarid Mediterranean regions: An approach using Landsat images in northeast Spain, *Remote Sensing of Environment* 124 (2012) 1–14. doi:10.1016/j.rse.2012.04.023.
- [34] C. E. de Toledo, J. C. de Araújo, C. L. de Almeida, The use of remote-sensing techniques to monitor dense reservoir networks in the Brazilian semiarid region, *International Journal of Remote Sensing* 35 (10) (2014) 3683–3699. doi:10.1080/01431161.2014.915593.